Letter

Surface Review and Letters, Vol. 4, No. 1 (1997) 1–8


# IMAGING SURFACE STRUCTURES BY DIRECT PHASING

L. D. MARKS and R. PLASS
*Department of Materials Science and Engineering, Northwestern University, Evanston, IL 60208, USA*

D. DORSET
*Hauptman-Woodward Medical Research Institute, Inc, 73 High St, Buffalo, New York 14203-1196, USA*

Received 11 June 1996

We report success in applying direct phasing methods to produce images of surface structures at the atomic scale from intensity data collected using transmission electron diffraction.



## 1. Introduction

A major problem for fields as diverse as heterogeneous catalysis and electronic device fabrication is the atomic scale structure of surfaces. While there exist techniques using low energy electron diffraction (LEED) (see e.g. Ref. 1), transmission electron diffraction[2–8] or x-ray diffraction (see e.g. Refs. 9, 10) to refine a structure, it is often difficult if not impossible to solve from scratch without additional information. This is because, as in three-dimensional structure problems, it is easy to refine but difficult to determine a viable initial estimate. We report here success in applying direct phasing methods to produce images of surface structures at the atomic scale from intensity data collected using transmission electron diffraction. This result has the potential to make it relatively simple to solve surface structures in the future.

A major advance over the last decade has been images of surfaces from scanning tunneling microscopy (STM) (see e.g. Ref. 11). However, despite the many successes there have also been failures since STM probes the surface density of states rather than atomic positions. An example of relevance later is the gold-on-silicon (111) $\sqrt{3} \times \sqrt{3}$ R30 surface. While commonly believed to consist of gold trimers,[12] STM images see only a single feature per unit cell.[13–15] Thus there has been work developing alternative imaging techniques, for instance photoelectron holography (see e.g. Refs. 16, 17) and high resolution transmission electron microscopy.[3,6,8,18]

For the related problem of three-dimensional crystallography, it is now common to use direct methods (see e.g. Ref. 19) to determine the initial structure estimate. Primarily through the use of x-ray diffraction data but more recently from transmission electron diffraction,[20] it is now almost routine to determine the structure of large, complicated crystals.

Despite its proven power for three-dimensional structure solutions, whether it can be used for surfaces is not at all clear. In fact, there are major differences both in the character and the quality of the problem. For instance, in three dimensions atoms cannot overlap but in projection for a surface they can, which contradicts some of the fundamental assumptions of direct phasing techniques. It is also known that for the similar problem of phase restoration of aperiodic images, solutions exist in two dimensions but not in one;[21] by analogy the two-dimensional crystallographic phase problem may be less well defined than in three dimensions.

There are also issues due to the character of the experimental data. The surface lies on a substrate, and when surface and substrate reflections overlap it is almost impossible to differentiate the two. Consequently, all reflections which belong to the $1 \times 1$

lattice cannot be accurately measured. Since these may be large, the reciprocal space sampling can be very incomplete. Furthermore, with these reflections omitted the sampled surface potential need not be positive; the effective potential $V_e(\underline{r})$ for the measured intensities is related to the true one, $V(\underline{r})$, by

$$V_e(\underline{r}) = V(\underline{r}) - 1/n\Sigma V(\underline{r} - \underline{l})\,, \qquad (1)$$

where the sum is taken over the lattice vectors of the $1 \times 1$ lattice ($\underline{l}$) and $n$ is the multiplicity of the cell, e.g. 49 for $7 \times 7$. [This is for kinematical electron diffraction; for x-ray diffraction the potential would be replaced by the electron density $\rho(\underline{r})$.] This lack of positivity violates a basic premise of traditional direct methods (see e.g. Ref. 22). The potential is also not only due to simple atomic scatterers, but includes effects from subsurface strain fields which are more important at higher angles,[3,6] and can be quite substantial.

A further problem is that a large, accurate data set is required to achieve sufficient resolution in order to differentiate the atoms. This is difficult to achieve with current x-ray sources, although possible with transmission electron diffraction. However, here there are perturbations due to dynamical diffraction, although there is evidence[5,23,24] that these effects are small with symmetrized data provided that strong bulk diffraction is avoided.

Finally, it is rare that the number and type of atoms contributing to the diffraction is well defined. With a simple adsorbate structure the coverage of the adsorbed species may be quite well known, but the number of substrate atoms contributing to the scattering is almost impossible to determine *a priori*.

Here we will demonstrate using experimental data that despite these problems, direct methods can be used.

## 2. Experimental Methods

The data that we have used were for two surfaces: the $\sqrt{3} \times \sqrt{3}$ R30 Au-on-Si (111) surface (see e.g. Refs. 12–14) (p3 symmetry) and the $5 \times 2$ Au-on-Si (111) surface[25,27] (pm symmetry in a $10 \times 2$ cell); details of the experimental methods have recently been published.[7,8] For reference, diffraction patterns are shown in Fig. 1, and note that the $\sqrt{3} \times \sqrt{3}$ surface is known to have a coverage of approximately one monolayer of gold (three sites per unit cell), and the $5 \times 2$ about 0.4 (four sites in the $10 \times 2$ cell).

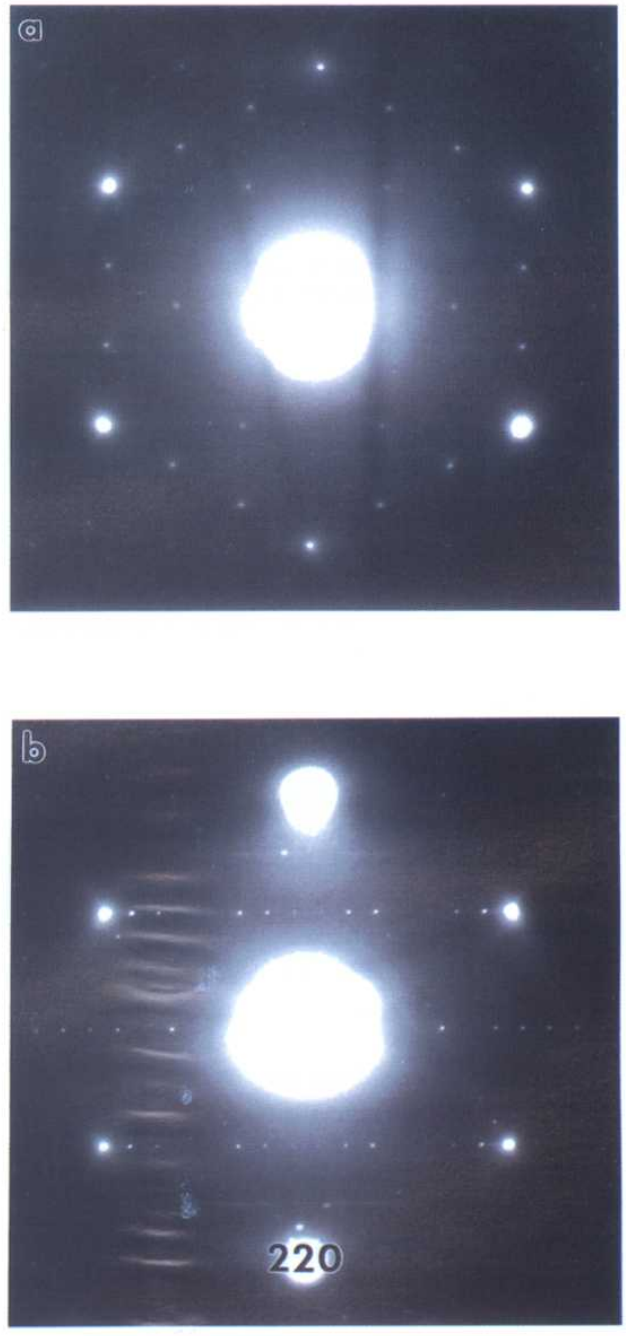


Fig. 1. Transmission electron diffraction patterns of (a) the $\sqrt{3} \times \sqrt{3}$ R30 surface and (b) the $5 \times 2$ surface.

## 3. Implementation of Direct Phasing

We initially worked with the $\sqrt{3} \times \sqrt{3}$ surface with a blind test where the data obtained at Northwestern were passed to the Hauptman-Woodward Institute, the only other information provided being that the unit cell contained three gold atoms and three or more silicons. A Wilson plot[28] was made to evaluate the overall temperature factor, but no evidence was found for a temperature falloff (i.e. $B = 0.0$ Å$^2$), indicating the presence of subsurface strains.[3,6]

To calculate normalized structure factors $|E(\underline{g})|$, the data resolution was limited to 1.00 A$^{-1}(\sin\theta/\lambda)$, yielding, for the first data set examined, 51 unique reflections. These were arranged in order of the decreasing $|E(\underline{g})|$ value for the calculation of $\Sigma_2$ three-phase invariant sums,[29] so the most optimal sequence of phase determination could be ascertained via a test of convergence.[30] It was seen that the phases of the largest $|E(\underline{g})|$ reflections, (2,1) and (1,2), could be linked to phase 49/51 unique terms.

Since there are no permitted origin-defining reflections for this plane group,[31] i.e. all hk reflections are phase invariants, the phase determination was carried out via the Sayre–Hughes equation[32,33] with an estimate of the $E(\underline{0})$ term set at $\sqrt{N}$, where $N$ is the number of atoms in the unit cell. Algebraic phase values were given to the (2,1) and (1,2) reflections and these were permuted through four quadrants of phase space (45°, −45°, 135°, −135°) to generate multiple trial solutions of seven



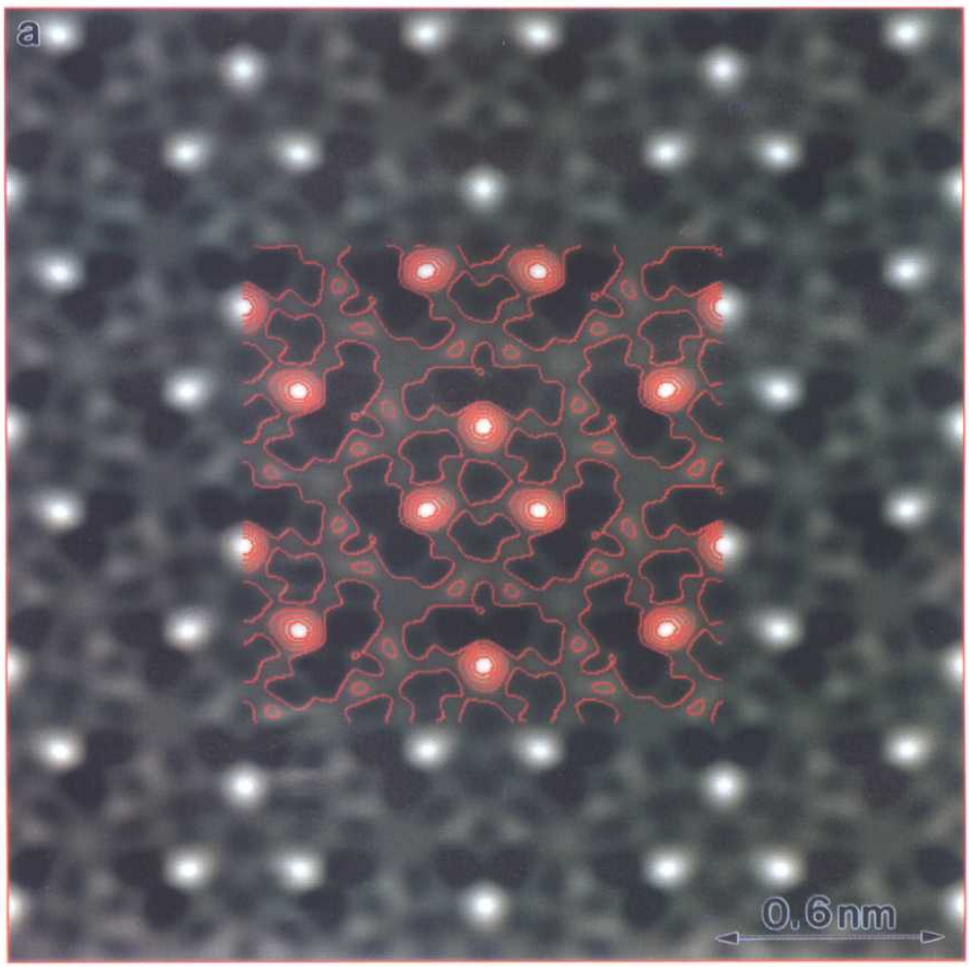


Fig. 2. The two possible solutions, (a) with the correct stoichiometry and (b) with only 1/3 of a monolayer, with contours superimposed in the central region. In both cases negative regions have been clipped, and black is the zero level. The poorly resolved silicon sites are arrowed.

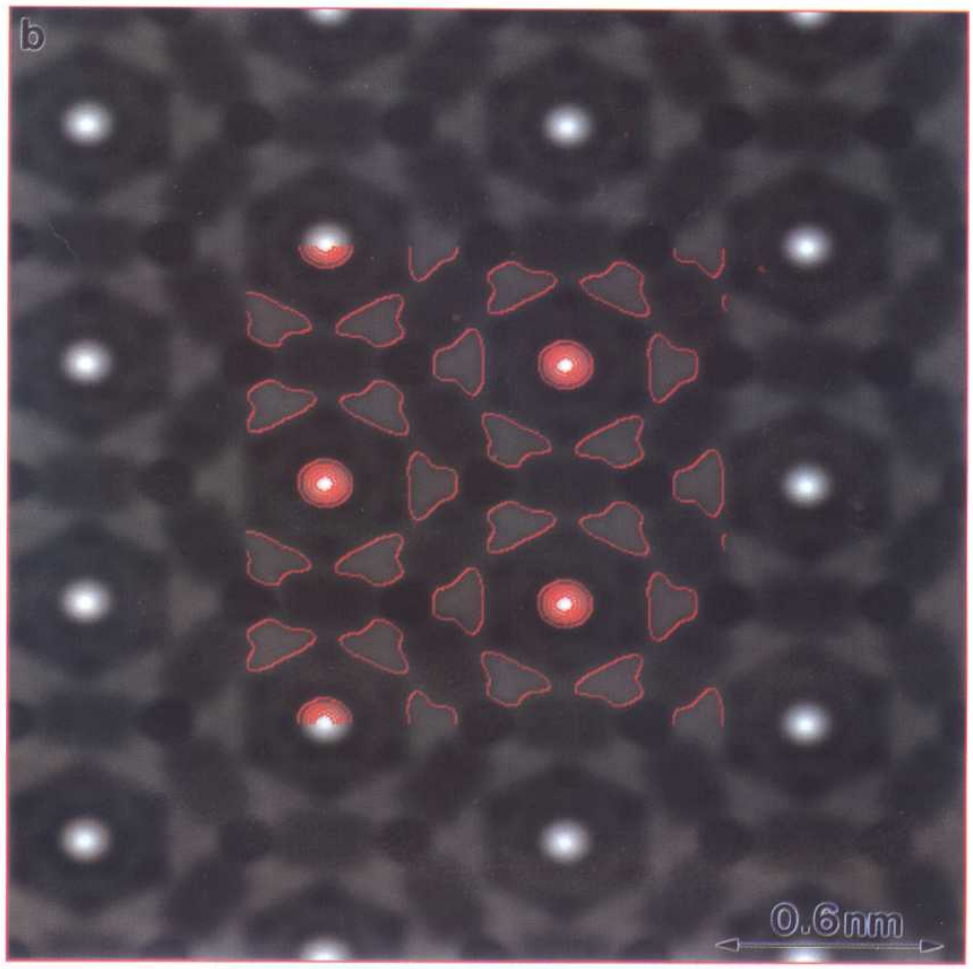


Fig. 2. (*Continued*)



reflections after one cycle of the phase convolution. From the resultant 16 trials, trial potential maps were generated and the density levels were monitored as an approximate indication of map "peakiness."[34] This was used as a figure of merit,[35] and two possible solutions were found (see Fig. 2).

Consequently a more detailed analysis was performed at Northwestern for both this surface and the $5 \times 2$. Good results were obtained using a minimum least squares solution of the Sayre equation. To be specific, a solution was sought that minimized

$$R^2 = \Sigma|F(g) - \alpha F_c(g)|^2/\Sigma|F(g)^2\,, \qquad (2)$$

where $F(g)$ are experimental structure factors for the reflection $g$, $\alpha$ is chosen to minimize this equation [thereby reducing sensitivity to errors in $F(\underline{0})$], and $F_c(g)$ the calculated structure factors from

$$F_c(g) = \{f(g)/W(g)\}\Sigma U(g-\underline{h})U(\underline{h})W(g-\underline{h})W(\underline{h})\,, \qquad (3)$$

with $U(g)$ the unitary structure factors and the "window function" $W(g)$ chosen to approximately satisfy

$$W(g) = \text{const} \times \Sigma W(g-\underline{h})W(\underline{h})\,, \qquad (4)$$

with the last sum taken over the intensities (measured and unmeasured) up to the cutoff. (As a consistency check we also monitored the related R factor using only the moduli of the structure factors. The results herein were also not sensitive to whether unitary or normalized structure factors were used.) The window function, which is comparable to weighting functions used in codes such as MULTAN, merits a little discussion. Numerically, a

simple Gaussian decay of $W(g) = \exp[-(g/g_{max})^2]$ was used, and serves the same purpose as windows applied to real data when one is estimating power spectra, i.e. it reduces ringing due to the data truncation (see e.g. Ref. 36); with it the RMS fractional error for Eq. (4) was about 1%, compared to 23% for a constant value of $W(g)$. Note that data truncation is a more severe effect in two dimensions than in three, and that the window will partially compensate for the decay in the atomic scattering factors. (Results without the windowing were noisier and noticeably inferior.)

Data sets to a particular cutoff in reciprocal space were produced and symmetrized, and only those beams larger than the maximum error of the measurement and the deviation between equivalent reflections were used. (This screens for beams strongly affected by dynamical scattering.) The Debye–Waller terms were estimated at one to two times the bulk values, which appears, from the data available to date, to be approximately correct. The raw data were normalized such that the sum of measured intensities was 1, and $F(\underline{0})$ taken as 1 prior to conversion to unitary structure factors.

For a rough estimation of likely solutions the two strong beams [(2,1) and (1,2)] were scanned in steps of 3° for the $\sqrt{3} \times \sqrt{3}$ structure. The tangent formula was used iteratively, terminating when the R factor increased. The final solutions were obtained through a full minimization using the routine dmnf from NETLIB.[37]



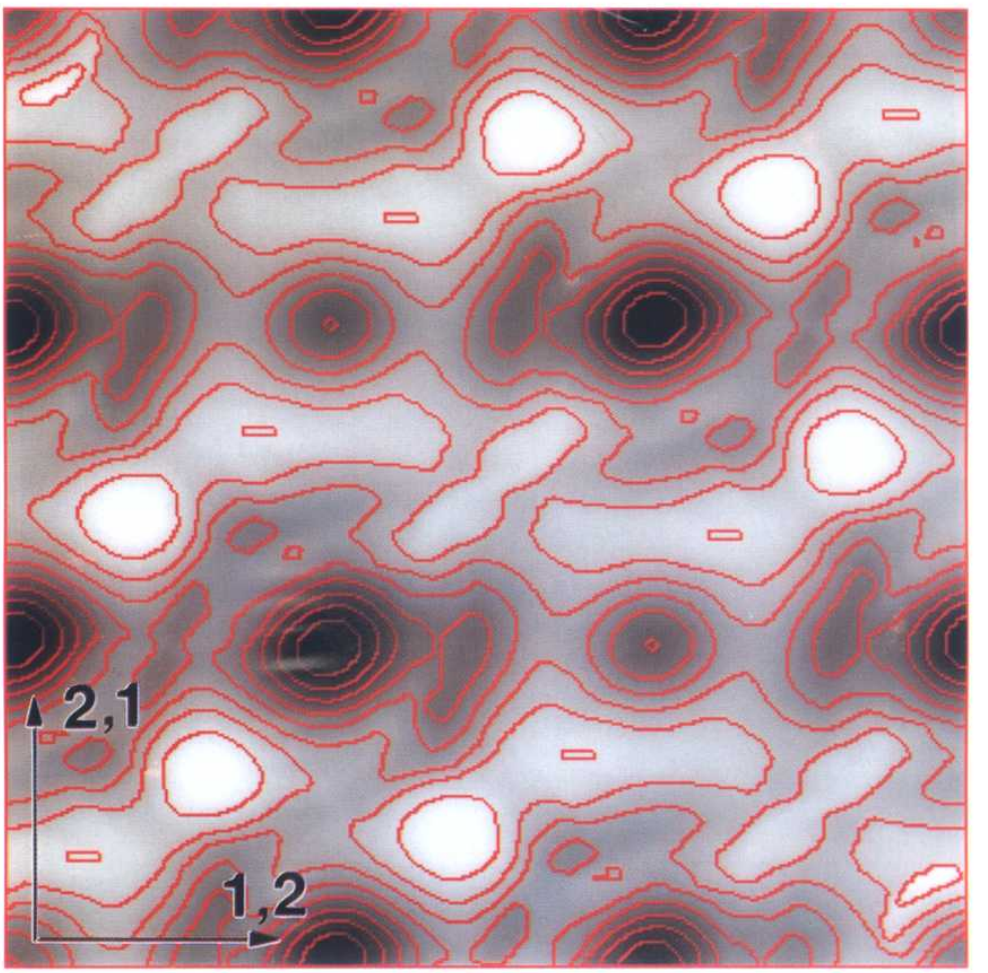


Fig. 3. Plot of the R factor with superimposed contours generated by scanning the (2,1) and (1,2) in 3° steps, with contours superimposed, with black corresponding to regions of a better R factor. The correct structure near 120, 120° is preferred to the solution with 120, 240°, corresponding to Figs. 2(a) and 2(b) respectively.

Figure 3 shows a plot of the R factor for a rough scan of the $\sqrt{3} \times \sqrt{3}$ surface with 3° steps in angles. There are only two possible solutions: one low R factor solution exists, and a second higher R factor solution; the formed has the correct stoichiometry while the latter does not. One independent gold atoms as well as two possible disordered silicon positions are present, which is consistent with a more sophisticated dynamical refinement.[7]

The $5 \times 2$ surface was not as simple, and a branching strategy was used. Using the strongest beam [the (13,2) and its equivalents] to fix the origin, we scanned first the (1,2) and (3,2) looking for minima in the R factor [Eq. (3)], thereby determining the approximate phase relationship:

$$(3,2) = (1,2)^*3 + \pi\,. \tag{5}$$

Using this as an algebraic equation for the (3,2) phase, and in a similar fashion building iteratively, we determined that

$$(11,2) = -2^*(1,2) + \pi \text{ or } 0\,, \tag{6}$$

$$(14,0) = (1,2) + \pi \text{ or } 0\,, \tag{7}$$

$$(16,0) = 3^*(1,2) + \pi \text{ or } 0\,. \tag{8}$$

With this number of beams defined it was possible to fix the (1,2) as having a value near to $2\pi n/6$ where values larger than $\pi$ were inverses, plus translationally equivalent sites. Data to 1.5 Å did not clearly resolve the gold, while those to 1 Å did. Full least squares refinements of the phases were attempted, but were unstable due to noise in the data.

Of the 32 possible solutions, about half could be immediately discarded as having a low kurtosis,[35]

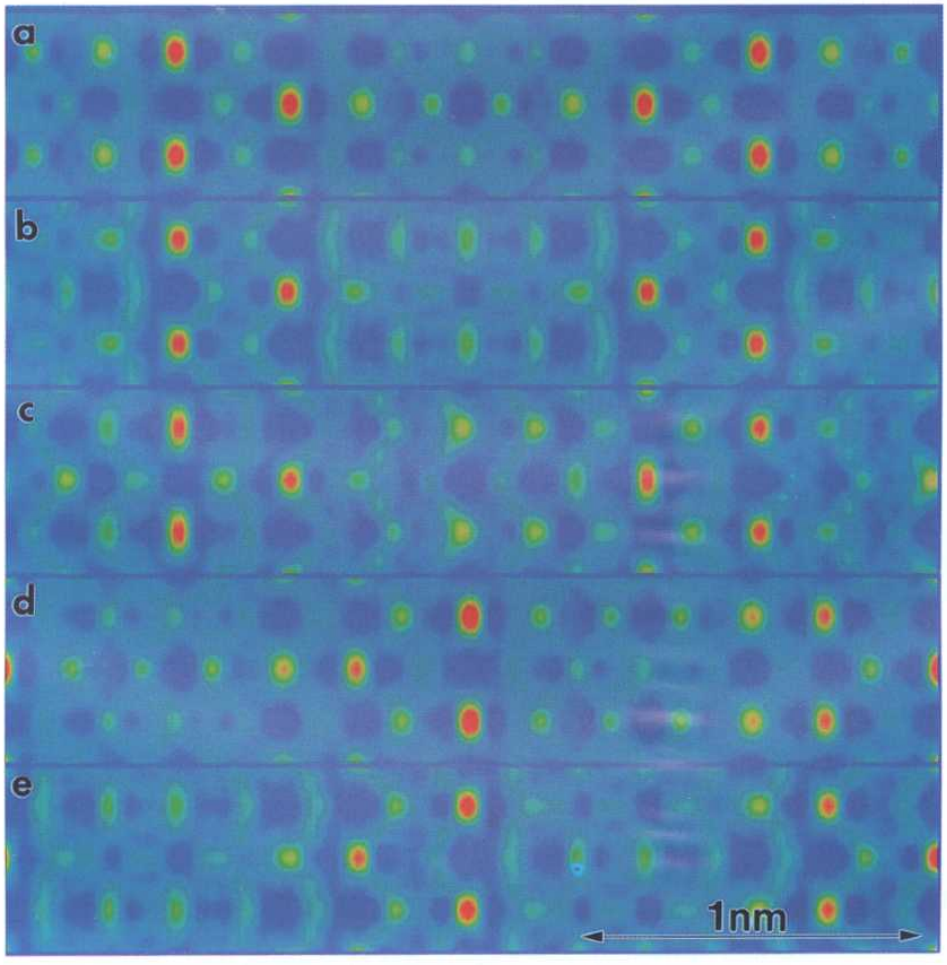


Fig. 4. Pseudocolor maps (red high and blue low) of the surface, all of which show a total of four gold sites and a very similar arrangements of silicon sites. (The intensity level of the gold has been truncated so that silicon is visible.)

as could some others which were not close to the correct stoichiometry. The remaining ones were all variations around a simple structure, as shown in Fig. 4. The gold atoms are shown clearly (red), and also some possible sites for the silicon (green). While not a full structure solution, there is certainly enough to determine the basic elements from which a $\chi^2$ refinement or heavy atom holography[8] could start. Note that the disorder in some of the silicon sites vertically cannot be ruled out; within the $10 \times 2$ cell the true structure has a disordered translational symmetry element (0.5, $\pm$0.25). This structure is not as well established as that of the $\sqrt{3} \times \sqrt{3}$, so the results herein provide the first corroborating evidence.

## 4. Discussion

In both cases it is apparent that good results which are very consistent with the structure of the surfaces are obtained. This implies that direct methods can be applied to general surface-crystallographic problems, particularly as data collection techniques improve. The $\sqrt{3} \times \sqrt{3}$ case is rather simple, with the gold locations well defined by the strong (2,1) and (1,2) beams. The silicon atoms are less well defined due to the lack of the $1 \times 1$ lattice point data, since they are only slightly displaced from bulk sites. The $5 \times 2$ case is a more stringent test, since it defeated earlier attempts to solve the structure using a Patterson function approach.[26] From HREM data we know that the (2,0) is very strong, but was occluded in the diffraction patterns by diffuse intensity around the transmitted beam. Furthermore, since (13,2) is very strong and (3,2) the second-strongest beams, it follows the (0,4) is also very strong as well as (10,0) and (15,2), all of which are coincident with bulk beams. This data set is thus rather incomplete, as well as having a much more complicated structure. The unit cell is also larger, and since the depth of strains scales with the in-plane size of the reconstruction, these perturbations will be larger.

We would be overstating the case to claim that in all cases simple approaches will lead to directly interpretable "images" of the surface such as we found for the two systems studied here. However, one does not need a complete image; only sufficient information to deduce reasonable starting points and exclude others. If only parts of the structure are resolved, this still may be more than adequate for "heavy atom holography"[9] or Karle recycling.[38] (As with any direct method the acid test is the $\chi^2$ from a final refinement.) More complicated structures such as the Si(111) $7 \times 7$ surface, which contains 102 atoms in a pseudo p6m unit cell (stricty, p3ml), are more challenging. We have numerically confirmed using simulated diffraction data that the true phases are a local minimum of the Sayre equation, but more work is required to explore in detail all the possible solutions.

One interesting point is whether techniques based upon the Sayre equation and the tangent formula are the best. Negative regions in the effective surface potential $[V_e(\underline{r})]$ become positive when the square is taken. Provided that there is little to no overlap between these peaks and the atomic sites, they will contribute only to the unmeasured intensities. There is no reason why one cannot consider the cube, to preserve the signs, or an exponential of the real space potential to generate new phases. (This is effectively equivalent to using the generalized tangent formula proposed by Karle.[39]) Numerical tests indicate that these give almost identical results, often smoother in angular scans (i.e. better-conditioned). Note that for certain surfaces the Sayre equation will define no new reflections whilst these alternatives would — for instance Si(001) $2 \times 1$, where only reflections satisfying $h = 2n + 1$ are measured. There may also be strategies for taking into account the subsurface strain effects, although this requires more work.

There is also no reason why the substrate should be ignored, at least for electron diffraction. If one arranges to study only the bottom surface, a better approximation to the exit wave would be

$$\psi(\underline{r}) = T(\underline{r}) \exp[i\sigma V(\underline{r})] = T(\underline{r})[1 + i\sigma V(\underline{r}) - \cdots], \tag{9}$$

where $T(\underline{r})$ is the wave just before the surface of interest. Since $T(\underline{r})$ can be measured and calculated rather well, it can be incorporated into the formulation of the problem. [Note that for the related problem of heavy atom holography,[8] inclusion of $T(\underline{r})$ gives substantially better results.]

While it is certain that more work needs to be done, the future looks promising for direct method solutions of surface-crystallographic problems.

## Acknowledgments

This research was supported by the National Science Foundation and the Air Force Office of Scientific Research.

## References

1. M. A. Van Hove, W. Moritz, H. Over, P. J. Rous, A. Wander, A. Barbieri, N. Materer, U. Starke and G. A. Somorjai, *Surf. Sci. Rep.* **19**, 191 (1993).
2. K. Takayanagi, Y. Tanishiro, S. Takahashi and M. Takahashi, *Surf. Sci.* **164**, 367 (1985).
3. L. D. Marks, P. Xu and D. N. Dunn, *Surf. Sci* **294**, 324 (1993).
4. G. Jayaram, P. Xu and L. D. Marks, *Phys. Rev. Lett.* **71**, 3489 (1993).
5. R. D. Twesten and J. M. Gibson, *Ultramicroscopy* **53**, 223 (1994).
6. G. Jayaram, R. Plass and L. D. Marks, *Interface Science* **2**, 381 (1995).
7. R. Plass and L. D. Marks, *Surf. Sci.* **342**, 233 (1995).
8. L. D. Marks and R. Plass, *Phys. Rev. Lett.* **75**, 2172 (1995).
9. D. Dornisch, W. Moritz, H. Schulz, R. Feidenhans'l, M. Nielsen, F. Grey and R. L. Johnson, *Phys. Rev.* **B44**, 11221 (1992).
10. Y. Kuwahara, S. Natani, M. Takahsi, M. Aono and T. Takahashi, *Surf. Sci.* **310**, 226 (1994).
11. G. Binning, H. Rohrer, Ch. Gerber and E. Weibel, *Phys. Rev. Lett.* **49**, 57 (1982).
12. M. Chester and T. Gustafsson, *Surf. Sci.* **256**, 135 (1991).
13. J. Nogami, A. A. Baski and C. F. Quate, *Phys. Rev. Lett.* **65**, 1611 (1990).
14. T. Takami, D. Fukushi, T. Nakayama, M. Uda and M. Aono, *Jpn. J. Appl. Phys.* **33**, 3688 (1994).
15. Y. G. Ding, C. T. Chan and K. M. Ho, *Surf. Sci. Lett.* **275**, L691 (1992).
16. D. K. Saldin, G. R. Harp, B. L. Chen and B. P. Tonner, *Phys. Rev.* **B44**, 2480 (1992).
17. C. S. Fadley, *Surf. Sci. Rep.* **19**, 231 (1993).
18. P. Xu, D. Dunn, J. P. Zhang and L. D. Marks, *Surf. Sci. Lett.* **285**, L479 (1993).
19. M. M. Woolfson, *Acta Cryst.* **A43**, 593 (1987).
20. D. L. Dorset, *Structural Electron Crystallography* (Plenum, New York, 1995).
21. R. H. T. Bates and M. J. McDonnell, *Image Restoration and Reconstruction* (Clarendon, Oxford), pp. 108–114.
22. J. Karle and H. Hauptman, *Acta Cryst.* **3**, 181 (1950).
23. Y. Tanishiro and K. Takayanagi, *Ultramicroscopy* **27**, 1 (1989).
24. L. D. Marks, T. S. Savage, J. P. Zhang and R. Ai, *Ultramicroscopy* **38**, 343 (1991).
25. J. D. O'Mahony, C. H. Patterson, J. F. McGilp, F. M. Leibsle, P. Weightman and C. F. J. Flipse, *Surf. Sci. Lett.* **277**, L57 (1992).
26. Ch. Schamper, W. Moritz, H. Schulz, R. Feidenhans'l, M. Nieslen, F. Grey and R. L. Johnson, *Phys. Rev.* **B43**, 12130 (1991).
27. L. E. Berman, B. W. Batterman and J. M. Blakely, *Phys. Rev.* **B38**, 5397 (1988).
28. A. J. C. Wilson, *Nature* **150**, 151 (1942).
29. H. A. Hauptman, *Crystal Structure Analysis: The Role of the Cosine Seminvariants* (Plenum, New York, 1972).
30. M. Woolfson and H.-F. Fan, *Physical and Non-physical Methods of Solving Crystal Structures* (Cambridge University Press, Cambridge, 1995), pp. 103–104.
31. D. Rogers, in *Theory and Practice of Direct Methods in Crystallography*, eds. M. F. C. Ladd and R. A. Palmer (Plenum, New York, 1980), pp. 23–92.
32. D. Sayre, in *Theory and Practice of Direct Methods in Crystallography*, eds. M. F. C. Ladd and R. A. Palmer (Plenum, New York, 1980), pp. 271–286.
33. E. W. Hughes, *Acta Cryst.* **6**, 871 (1953).
34. E. Stanley, *Acta Cryst.* **A42**, 297 (1986).
35. W. Cochran, *Acta Cryst.* **5**, 65 (1952).
36. W. Press, S. A. Teukolsky, W. T. Vetterling and B. P. Flannery, *Numerical Recipes* (Cambridge University Press, Cambridge, 1992), pp. 545–551.
37. G. W. Stewart, *J. Assoc. Comput. Mach.* **14**, 72 (1967); see http://www.netlib. org.
38. J. Karle, *Acta Cryst.* **B24**, 182 (1968).
39. J. Karle, *Acta Cryst.* **B27**, 2063 (1971).